https://doi.org/10.5194/egusphere-2025-3461
Preprint. Discussion started: 15 December 2025

MATILDA-Online v1.0.1: A Cloud-based Open-Source Workflow for Modeling Water Resources in Glacierized Catchments

Phillip Schuster[1,*], Ana-Lena Tappe[1], Alexander Georgi[1], Christoph Schneider[1], Mia Janzen[1], and Tobias Sauter[1]

[1]Geography Department, Humboldt-Universität zu Berlin, Berlin, Germany
[*]Corresponding Author

Correspondence: Phillip Schuster (phillip.schuster@geo.hu-berlin.de)

Abstract. The mountain cryosphere is a linchpin of global water security. Changes in high mountain systems due to climate change are putting the freshwater resources of almost a quarter of the world's population at risk. Hydrological modeling is the foundation for developing mitigation and adaptation strategies, supporting policy and water management decisions, and preventing water-related conflicts. However, many vulnerable regions lack access, resources, and training to implement advanced (glacio-)hydrological modeling in decision-making and resource management processes. The open-source Toolkit for Modeling glacier evolution and wATer resources In meso-scale gLacierizeD cAtchments (MATILDA) provides a cloud-based modeling workflow that allows users to generate scenario-based projections and analyze runoff contributions in glacierized catchments. A combination of a temperature-index melt model, an updated Δh routine for glacier evolution, and the HBV hydrological model is forced with open-access datasets provided via cloud services and complemented by a set of processing tools. MATILDA is published as a Jupyter Book on a self-contained website, allowing easy access to the entire processing chain from data acquisition and model calibration to scenario generation and output analysis in a user-friendly Python environment. This paper is the first of a two-part publication outlining the general workflow, describing input data and modeling routines, and assessing parameter sensitivity. The second part demonstrates the application in a case study and discusses the uncertainty in the projections.

1 Introduction

Climate change and water security have moved from the realm of scientific debate to the core of the global security discourse (Vishwanth, 2019). The 2015 World Economic Forum in Davos ranked the water crisis as the top risk facing societies (WEF, 2015). Eight years later, the direct impacts of climate change and the failure of mitigation and adaptation strategies hold the top 3 positions of the ranking (WEF, 2023). Nearly a quarter of the world's population is directly dependent on freshwater from high mountain headwaters (Immerzeel et al., 2020), making the mountain cryosphere a linchpin of water security. Glaciers and seasonal snowpack serve as critical drought-resilient water reservoirs, mitigating inter- and intra-annual variations in precipitation and evaporation by storing solid precipitation and releasing it during warmer periods (Hagg et al., 2007; Pohl et al., 2017; Pritchard, 2019). Therefore, changes in the mountain cryosphere have major impacts on downstream societies

https://doi.org/10.5194/egusphere-2025-3461
Preprint. Discussion started: 15 December 2025

(Hock et al., 2019; Viviroli et al., 2020; Immerzeel et al., 2020; Aggarwal et al., 2022). In the course of ongoing global warming, glaciers worldwide have experienced rapid mass loss (Zemp et al., 2019; Hock et al., 2019), which is projected to continue regardless of anthropogenic greenhouse gas emission pathways (Miles et al., 2021; Rounce et al., 2020). Under these conditions, integrated water management and governance across all scales is necessary but challenging and requires strong scientific support (Chen et al., 2018; Hock et al., 2019). Assessment of hydrological cycles and their short- and long-term projections are crucial to develop mitigation and adaptation strategies, support policy and water management decisions, and prevent water-related conflicts (Hock et al., 2019; Barandun et al., 2021; Schaffhauser et al., 2023).

Since the advent of computers in environmental science, numerous hydrological models have been developed and the number is increasing fast (Clark et al., 2011; Horton et al., 2022). However, while computational times (Kim and Ryu, 2019), data availability (Winsemius et al., 2009; Tarek et al., 2020; Yin et al., 2021; Ali et al., 2023) and therefore model robustness (Finger et al., 2015; Birhanu et al., 2018) have improved significantly, very few models have made the step into regular application in countries of the Global South. While most developing countries have limited modeling expertise and technical capabilities to establish their own standard models (Alcantara et al., 2019; Paul et al., 2021), the international scientific community may assist in compensating for this. In accordance with the UNESCO's Recommendation on Open Science adopted by 193 countries in 2021 (UNESCO, 2021), a large number of dedicated researchers, institutions, and cloud service providers has created a variety of open-access datasets and open-source services. However, the standard application of sophisticated hydrologic and climate modeling for decision making and resource management is still mostly limited to developed countries. Very few tools provide the low access and computational costs needed to engage management professionals and stakeholders in the regions where they are most needed (Photiadou et al., 2021).

Web-based applications following the Hydrologic Modeling as a Service (HMaaS) approach can compensate for deficiencies in technical resources and expertise (Alcantara et al., 2019; Gan et al., 2020; Photiadou et al., 2021). By increasing accessibility to sophisticated models, they can facilitate their integration at the local level, enhancing decision-making capabilities (Brooking and Hunter, 2013; Biswas and Hossain, 2018; Alcantara et al., 2019). While there have been several publications on web-based hydrological tools, most of them are either limited to a specific region (Alcantara et al., 2019; De Filippis et al., 2022) with a strong focus on developed countries (Donnelly et al., 2016; Lew et al., 2022) or are designed for short and medium term forecasts for flood and/or drought warnings (Alfieri et al., 2013; Sanchez Lozano et al., 2021; De Filippis et al., 2022). Other services focus on only parts of the modeling process, such as data acquisition from web sources (Gichamo et al., 2020) and data exchange (e.g. www.hydrosheds.org and www.cuahsi.org/data-services/hydroshare) or parameter autocalibration (Rajib et al., 2022). Some fully-integrated tools provide a strong feature set for the complete workflow, but have technical barriers by not providing a user interface (Erazo Ramirez et al., 2022) or requiring client-side hosting (McDonald et al., 2019; Jadidoleslam et al., 2020; Ewing et al., 2022). In recent years, however, fully hosted applications with global coverage have been developed, offering a wide range of features for in-depth analysis of climate-change impacts on local hydrology for any given region. While these tools may be promising, at the time this study was submitted, they either did not allow interactive modeling of user-defined catchments (Arheimer et al., 2020) or were not (yet) available to the public (Taylor et al., 2021). Furthermore, all of the aforementioned tools are designed for lowland areas. They either neglect glacier melt entirely or do not allow for

https://doi.org/10.5194/egusphere-2025-3461
Preprint. Discussion started: 15 December 2025

scenario-based projections. Thus far, we are unaware of an open-source, open-access, server-side modeling tool that allows users to acquire data and calibrate and evaluate a hydrological model for a custom climate change impact assessment at the catchment scale in areas dominated by melt water.

Initiated in a Kyrgyz-German research collaboration, we have compiled an open-source toolkit for **M**odeling glacier evolution and w**AT**er resources **I**n meso-scale g**L**acierize**D** c**A**tchments (MATILDA). It consists of well-established modeling routines and a set of tools, forced with open-access datasets provided via cloud services. Designed as a user-friendly online workflow in Python, documented in Jupyter notebooks, MATILDA provides a streamlined process from data acquisition and preprocessing through calibration, parameter optimization, analysis, and interactive visualization. Users can generate scenario-based hydrological projections and interactively analyze trends in runoff contribution. The tool can be run with default parameters or calibrated to user-provided runoff observations. With this approach, we aim to provide an easy access to modern routines, platforms, and tools to local professionals, while also targeting students, and fellow researchers.

This study is the first of a two-part publication. Here we outline the general structure of the MATILDA workflow, describe input data and modeling routines, and assess parameter sensitivity. The second part presents a case study that demonstrates the application of the tool in practice and discusses uncertainties and improvement potential.

2 Model description

The main part of the MATILDA workflow is released as a standalone Python package comprising two components: (1) `matilda.core` and (2) `matilda.mspot`. The former contains the core modeling routines, while the latter is responsible for the statistical parameter optimization. The core model is a semi-distributed conceptual catchment model based on the renowned HBV model (Bergström, 1976; Seibert and Vis, 2012) and an updated version of the Δh **parametrization** proposed by Seibert et al. (2018) to account for glacier evolution. With a discharge time series and the corresponding coordinates as the minimum user input for calibration, it allows the simulation of any given catchment from 1979 to 2100 in daily resolution. To reduce download volume and calibration time, all input data are aggregated into at least two sub-catchments: the glacierized and the ice-free part. Each of these parts is handled by a dedicated module, complemented by auxiliary modules for pre-processing and output analysis. For additional sub-catchments, the user can setup multiple instances of the core model and customize calibration.

Figure 1 illustrates the key processes modeled and the associated parameter names. Detailed descriptions and default values are listed in Table 1. Unless otherwise noted, all reservoirs and fluxes in the following are consistent in millimeter water equivalent (mm w.e.). Model parameters are in regular style, while all other variables are in italics.

2.1 Glacial modeling

Glacier evolution in the catchment is modeled using three primary routines: (1) A basic **temperature index model** (Hock, 2003; Seibert and Vis, 2012) calculates the snowpack evolution and returns daily ice and snow melt rates. Solid precipitation is added to the snowpack, while snowmelt decreases it. Melt is proportional to the positive degree-days (PDD) which are the

https://doi.org/10.5194/egusphere-2025-3461
Preprint. Discussion started: 15 December 2025

daily (t) temperature excess T above a threshold TT_{snow} given as

$$PDD(t) = \max(T(t), \mathrm{TT}_{snow}). \tag{1}$$

The potential melt M_{pot} is calculated by

$$M_{pot}(t) = PDD(t) \cdot \mathrm{CFMAX}_{snow}, \tag{2}$$

where CFMAX_{snow} is snow melt parameter in mm K^{-1} d^{-1} . The actual snow melt

$$M_{snow}(t) = \min(SWE(t), M_{pot}(t)) \tag{3}$$

is limited by the amount of available snow water equivalent on the glacier SWE, while ice melt

$$M_{ice}(t) = (M_{pot}(t) - M_{snow}(t)) \cdot \frac{\mathrm{CFMAX}_{ice}}{\mathrm{CFMAX}_{snow}} \tag{4}$$

is proportional to excess snow melt. To account for differences in albedo between ice and snow, the melt parameter for ice CFMAX_{ice} is higher than the parameter for snow CFMAX_{snow} by a calibration factor CFMAX_{rel} between 1.2 and 2.5.

The fraction of melt water refreezing in the snowpack and on moulin walls is determined by the factor CFR. Both, the refreezing melt water

$$R_R(t) = M_{snow}(t) \cdot \mathrm{CFR}, \tag{5}$$

and the solid precipitation P_{solid} are finally subtracted from the total melt

$$M_{tot}(t) = M_{snow}(t) + M_{ice}(t) \tag{6}$$

to determine the annual surface mass balance

$$SMB = \sum_{t=1}^{A} P_{sol}(t) - M_{tot}(t) + R_R(t) \tag{7}$$

over the time period A. The code is based on the positive-degree model for Python (PyPDD) by Seguinot (2019).

(2) To account for seasonal variations in retention times, we use the **glacier storage-release scheme** proposed by Stahl et al. (2008) and included in the HBV.IANIGLA model by Toum et al. (2021). The delayed glacier runoff

$$Q_G(t) = KG(t) \cdot S_G(t) \tag{8}$$

https://doi.org/10.5194/egusphere-2025-3461
Preprint. Discussion started: 15 December 2025

depends on the liquid water stored in the glacier $S_G(t)$ and the time-varying outflow coefficient

$$KG(t) = KG_{min} + d_{KG} \cdot \exp[-\frac{SWE(t)}{(10^5)^{AG}}], \tag{9}$$

where KG_{min} is the minimum outflow representing winter conditions with a maximum snowpack and little glacial drainage (set at $KG_{min} = 0.1$ d^{-1}), while d_{KG} is the maximum outflow increase, with $KG_{min} + d_{KG}$ representing late summer conditions with minimum or no snowpack and maximum glacial drainage (set at $d_{KG} = 0.9$ d^{-1}). $SWE(t)$ is the water stored in the time-varying snowpack on the glacier, while AG is the calibration parameter (mm^{-1}) with high values resulting in small storage and immediate release, and low values extending the storage and delaying release.

(3) To account for changing glacier extent under future climate, a Δh **parameterization** is applied, following Seibert et al. (2018). The method uses glacier size-dependent mass-area coefficients from Huss et al. (2010) to update glacier area and thickness annually based on modeled mass changes. This approach has been shown to provide robust estimates of glacier evolution in hydrological models (Huss et al., 2010; Duethmann et al., 2015; Seibert et al., 2018). Using gridded ice thickness data from Farinotti et al. (2019), a basin-wide ice mass profile is created at 20 m elevation bands. Glacier melt is simulated from the initial state to a state with no ice, generating a look-up table of distributed glacier mass estimates with elevation bands as columns and melting steps of 1 % as rows. Based on the annual SMB values provided by the temperature index model, the glacier state between 0–100 % is determined. The respective row in the look-up table and the empirical glacier mass-area coefficients from Huss et al. (2010) allow then to update glacier area and distribution for the next year. The detailed procedure is described in Seibert et al. (2018). However, the method assumes glacier extents do not exceed their initial state. Since few glaciers show positive mass balance trends and MATILDA is designed for long-term analysis, we adapted the routine to retain any mass above 100% and apply it in later years when glacier extent drops below the initial level. While this may affect individual years, it conserves long-term accumulation.

Small glaciers at high elevations may stabilize above the regional equilibrium line altitude (ELA, Huss and Fischer 2016). In addition, despite warming trends, increasing precipitation may lead to increasing glacier area at high elevations (Zhang et al., 2019). We have modified the Δh routine to account for both of these effects. This modification allows to recalculate the average glacierized and ice-free catchment elevations based on the updated ice distribution. All elevations e are given in m a.s.l. and all area values a are given in km^2. For each year, we first determine the fractional glacierized area

$$a_{i,frac} = \frac{a_i}{\sum_{i=1}^{N} a_i} \tag{10}$$

within each elevation zone i on the catchment's total glacierized area $\sum_{i=1}^{N} a_i$. The average glacier-covered elevation

$$e_{glac} = \sum_{i=1}^{N} e_i \cdot a_i \tag{11}$$

is obtained by weighting the mean elevation of each zone e_i with the glacier-covered fraction $a_{i,\text{frac}}$. From the respective area and mean elevation values for the whole catchment and its (updated) glacierized fraction, we then derive the (updated) mean

https://doi.org/10.5194/egusphere-2025-3461
Preprint. Discussion started: 15 December 2025

elevation of the ice-free fraction

$$e_{non-glac} = \frac{e_{cat} \cdot a_{cat} - e_{glac} \cdot a_{glac}}{a_{cat} - a_{glac}}, \tag{12}$$

where e_{cat} and e_{glac} are the mean elevations of the whole catchment and the glacierized fraction respectively, and a_{cat} and a_{glac} are the corresponding area values.

2.2 Hydrological modeling

The hydrological module uses the HBV model (Bergström, 1976) in a lumped adaptation of HBV-light (Seibert and Vis, 2012) as implemented in the Lumped Hydrological Models Playground (LHMP) by Ayzel (2016). A spinup period of typical two years provides arrays of initial values for the following seven components ("boxes"): snowpack, snowmelt, soil moisture, upper and lower groundwater, actual evapotranspiration, and runoff. The snow routine adds solid precipitation to the snowpack SWE and calculates melt and refreezing using the temperature index approach (see 2.1). While a fraction of the total snow melt M_{snow} is retained in the snowpack, determined by the parameter CWH, the rest is added to the liquid precipitation P_{liquid} to form the recharge flux to the soil box

$$R_s(t) = M_{snow}(t) - (\text{CWH} \cdot SWE(t)) + P_{liq}(t). \tag{13}$$

The flux from the soil to the groundwater is calculated as

$$R_g(t) = \left(\frac{SM(t)}{\text{FC}}\right)^{\text{BETA}}, \tag{14}$$

where SM is the current soil moisture, FC is the maximum soil moisture storage, and BETA is a nonlinear shape coefficient (Bergström and Lindström, 2015). According to Seibert and Vis (2012), the loss of soil moisture due to evaporation

$$E_{act}(t) = E_{pot}(t) \cdot min\left(\frac{SM(t)}{\text{FC} \cdot \text{LP}}, 1\right), \tag{15}$$

and thus is limited by the amount of available SM, FC, and the evaporation control parameter LP. The potential evaporation is calculated by

$$E_{pot}(t) = (1 + \text{CET} \cdot (T(t) - T_M)) \cdot E_{pot,M}, \tag{16}$$

$$E_{pot} = \begin{cases} E_{pot}, & \text{if } E_{pot} > 0 \\ 0, & \text{otherwise} \end{cases} \tag{17}$$

where T_M is the long-term mean of T, CET is a evaporation correction parameter, and $E_{pot,M}$ is the long-term mean potential evaporation for day t (Seibert and Vis, 2012; Lindström and Bergström, 1992). If the potential evaporation is not

https://doi.org/10.5194/egusphere-2025-3461
Preprint. Discussion started: 15 December 2025

calculated by default (see eq. 22), but provided as input data, it is corrected by the deviations of the air temperature $T(t)$ from the long-term mean T_M for day t (Seibert and Vis, 2012; Lindström and Bergström, 1992). The percolation parameter PERC controls percolation from the upper groundwater box SUZ to the lower groundwater box (Seibert and Vis, 2012)

$$SLZ(t) = SLZ(t-1]) + \min(SUZ(t), \text{PERC}). \tag{18}$$

Finally, the runoff

$$Q_g(t) = \text{K}_0 \cdot \max(SUZ(t) - \text{UZL}, 0) + \text{K}_1 \cdot SUZ(t) + \text{K}_2 \cdot SLZ(t) \tag{19}$$

is calculated as the sum of three outflow components simulating different retention times. They are controlled by their individual recession coefficients ($\text{K}_0, \text{K}_1, \text{K}_2$) and the threshold parameter for the upper groundwater box UZL (Seibert and Vis, 2012).

To reduce noise in the simulated runoff Q_{sim} and control the delay, a Butterworth low-pass filter for discrete data (Zieliński 2021, Eq. 8.37) is applied (Ayzel, 2016), using the general transfer function

$$H(z) = \frac{b_0 + b_1 z^{-1} + \ldots + b_N z^{-N}}{1 + a_1 z^{-1} + \ldots + a_N z^{-N}}, \tag{20}$$

where z is the complex frequency variable, $b = [b_0, b_1, \ldots, b_N]$ are the coefficients of the numerator polynomial, $a = [a_1, \ldots, a_N]$ are the coefficients of the denominator polynomial, and N is the filter order. The `scipy.signal.butter` function allows to compute polynomial arrays for b and a by specifying a filter order N and a cutoff angular frequency w_c. By fixing both with the filter parameter MAXBAS as $N = \text{MAXBAS}$ and $w_c = \frac{1}{\text{MAXBAS}}$, we obtain the following transfer function to compute the smoothed simulated runoff Q_{sim} at time step t.

$$\begin{aligned} Q_{sim}(t) = \; & b_0 \cdot Q_g(t) + b_1 \cdot Q_g(t-1) + \ldots + b_{MAXBAS} \cdot Q_g(t - \text{MAXBAS}) \\ & - a_1 \cdot Q_{sim}(t-1) - \ldots - a_{MAXBAS} \cdot Q_{sim}(t - \text{MAXBAS}) \end{aligned} \tag{21}$$

3 Technical Implementation

MATILDA-Online is published as a self-contained website using the Jupyter Book format (Holdgraf et al., 2019), combining code cells, markdown, images, and interactive elements. Code is hidden by default, offering non-technical users easy access while supporting reproducibility – a key concern in hydrological studies (Stagge et al., 2019). With the click of a button, an online Python environment by mybinder.org (Project Jupyter et al., 2018) launches, allowing for a browser-based application on the example site or any other catchment.

Figure 2 summarizes the workflow and its modules. To reduce client-side computation and ensure global coverage, MATILDA uses cloud services like Google Earth Engine (GEE; Gorelick et al., 2017) for data input and preprocessing. The workflow consists of eight interactive Jupyter notebooks:

- Notebook 0: Introduction and GEE registration
- Notebook 1: Catchment delineation and static data

https://doi.org/10.5194/egusphere-2025-3461
Preprint. Discussion started: 15 December 2025

- Notebook 2: Climate reanalysis data
- Notebook 3: Climate projection data
- Notebook 4: Model calibration
- Notebook 5: Scenario runs
- Notebook 6: Interactive analysis, Climate impact assessment, and summary

3.1 Data and Preprocessing

MATILDA utilizes seven input datasets, with the user only required to provide runoff observations for calibration. GEE is accessed via its Python API packages `ee` (GEE, 2025) and `geemap` (Wu, 2020), which provide access to historical and future climate forcing data and the digital elevation model (DEM). The remaining datasets are obtained from other sources.

3.1.1 Static data

By default, MATILDA uses the 90 m resolution MERIT Hydro DEM, which is optimized for hydrological applications (Yamazaki et al., 2017). If desired, alternative DEMs hosted on GEE can be selected in the configuration file. After the user defines the gauge location, the catchment is delineated using the `pysheds` library (Bartos, 2020).

3.1.2 Glacier data

The catchment is assigned to a region in the Randolph Glacier Inventory 6.0 (RGI 6; RGI Consortium 2017). Glacier outlines from 2001 are downloaded, subset to the catchment, and refined to include only RGI polygons with >50 % overlap. Minor discrepancies are resolved by adjusting the catchment outline. The final outlines are stored in a `GeoPackage`. The area and mean elevation of the total and the glacierized sub-catchment are saved in the static `.yml` file. Initial ice mass is estimated from ice thickness rasters by Farinotti et al. (2019) and summarized in a `.csv` profile of total catchment ice mass (m.w.e.) by 10 m elevation bands.

3.1.3 Reanalysis data

Daily near-surface temperature and precipitation data from ERA5-Land (Muñoz Sabater et al., 2021) are accessed via GEE, enabling spatial and temporal subsetting with minimal downloads. The dataset is suitable for hydrological modeling (Probst and Mauser, 2022; Ougahi and Mahmood, 2022; Wu et al., 2023) and and may even provide long-term results comparable to actual observations (Tarek et al., 2020). To balance spatial heterogeneity and efficiency, all intersected ERA5-Land grid cells (0.01° x 0.01°) are aggregated using the area-weighted mean resulting in a single `.csv` of 1.4 MB with catchment-wide time series from 1979–2022. The reference elevation is calculated accordingly from the ERA5-Land geopotential height, converted to meters, and saved in the static `.yml` file. To facilitate the integration of observational data sets, we decided not to use

https://doi.org/10.5194/egusphere-2025-3461
Preprint. Discussion started: 15 December 2025

potential evaporation (PET) data from ERA5-Land, but to estimate it from air temperature as suggested by Oudin et al. (2005):

$$E_{pot} = \frac{R_e(T_{mean} + 5)}{\lambda 100}, \quad \text{if } T_{mean} + 5 > 0; \quad \text{else: } E_{pot} = 0, \tag{22}$$

where E_{pot} is the potential evaporation (mm day^{-1}), R_e is the extraterrestrial radiation at the latitude of the study area at a given julian day (MJ m^{-2} day^{-1}), T_a is the daily mean air temperature (°C), and λ is the latent heat flux which is considered equal to 2.45 MJ kg^{-1}. Oudin et al. (2005) show that this simple approach can be applied with comparable efficiency to more complex models such as the widely used Penman-Monteith model (Monteith, 1965; Allan et al., 1998; Oudin et al., 2005) while reducing the input data to a minimum.

3.1.4 Climate scenario data

Multi-model ensembles help reduce individual model uncertainty (Gholami et al., 2023; Wu et al., 2023). Therefore, the future climate impacts are simulated using 35 model simulations from the Climate Model Intercomparison Project Phase 6 (CMIP6, Eyring et al. 2016). The NEX-GDDP-CMIP6 dataset (Thrasher et al., 2022) accessed via GEE provides the data downscaled to 0.25° using a bias correction and spatial disaggregation method following (Wood et al., 2002, 2004) and manual trend adjustments. Area-weighted catchment averages of temperature and precipitation from 1950 to 2100 were downloaded for two Shared Socioeconomic Pathways (SSP2 and SSP5) and for the historical period prior to 2015. Multiprocessing allows for ensemble downloads in under two minutes under ideal server-side conditions. All 70 CMIP6 time series are bias-adjusted against ERA5-Land (1979–2022) using Scaled Distribution Mapping (SDM) via the `bias_correction` library (Kumar, 2022). This technique outperforms other quantile mapping methods in terms of preserving trends and predicting extreme events in raw GCM data (Switanek et al., 2017). As suggested by the authors, SDM is applied iteratively to discrete decades using a 30-year moving window (e.g. bias adjust 2021-2050 to receive 2031-2040, bias adjust 2031-2060 to receive 2041-2050 and so on). Finally, models with extreme outliers (>3 standard deviations) or abrupt changes (>5 K of annual mean temperature) are excluded. Both thresholds are configurable.

3.2 Calibration

The `matilda` package includes a calibration module (`matilda.mspot`) based on the `spotpy` library (Houska et al., 2015). It offers configurable optimization algorithms and objective functions that can be tailored to available computing resources and desired accuracy. The `matilda.core` model has a total of 21 non-optional parameters (see Table 1) of which 19 are HBV light standard parameters. Thus, the apparent risk of overparametrization must be mitigated by reducing the parameter space to decrease model uncertainty and equifinality, and enhance the forecast ability (Beven and Binley, 1992; Kuczera and Mroczkowski, 1998; Silvestro et al., 2015). The incorporation of additional objective functions (Her and Seong, 2018) and calibration parameters (Her and Chaubey, 2015; Finger et al., 2015) can reduce uncertainty in hydrological models. In glacierized catchments, the combination of snow data, runoff, and glacier surface mass balance observations (SMB) enhances model performance and process representation, while reducing equifinality and parameter uncertainty (Duethmann et al., 2014;

https://doi.org/10.5194/egusphere-2025-3461
Preprint. Discussion started: 15 December 2025

Finger et al., 2015; Nemri and Kinnard, 2020). This can avoid unrealistic melt rates (Stahl et al., 2008; Finger et al., 2015) and high sensitivity to climate forcing (Compagno et al., 2021). Consequently, MATILDA uses a four-step, hierarchical, process-based calibration, which is described in detail in Schuster et al. (2025d). Discharge observations and reference coordinates need to be provided by the user. By default, MATILDA uses SMB and snow water equivalent (SWE) datasets limited to High Mountain Asia (HMA). Additional areas will be included in the future and custom datasets can be added manually. Shean et al. (2020), provide average annual SMB (2000–2018) and uncertainty (σ) for 99 % of all glaciers in High Mountain Asia (HMA). MATILDA aggregates both to catchment-means, using $\mathrm{SMB}_{\mathrm{cat}} \pm \sigma_{\mathrm{cat}}$ as the calibration target. Users can simply replace this with a custom range. SWE estimates for 2000–2017 at 16 arcsecond (~500 m) resolution are sourced from the High Mountain Asia Snow Reanalysis (HMASR; Liu et al. 2021a). The dataset is based on a Bayesian reanalysis scheme of Margulis et al. (2019) assimilating seasonal snow cover from remote sensing with meteorological inputs (Liu et al., 2021b). The raw data requires preprocessing, which cannot currently be done in the online workflow (Schuster et al., 2025d). The corresponding scripts are provided via GitHub to be run locally.

3.3 Validation

Validation options largely depend on the regional data availability. While split-sample validation is standard (Klemeš, 1986), some studies recommend using all available data for calibration (Arsenault et al., 2018; Shen et al., 2022) as the number of observations improves model performance and reduces uncertainty (Her and Chaubey, 2015; Guo et al., 2020). Therefore, MATILDA allows flexible selection of calibration/validation periods. Additional validation (e.g., glacier change) can be added manually. Several validation options for a specific use case are provided in Schuster et al. (2025d).

3.4 Analysis and Visualization

Users can explore the projections in interactive figures using the `dash` library by `plotly` (Plotly Technologies Inc., 2015). Ensemble means including a 90% confidence interval (CI) of all `matilda.core` output variables can be plotted, customized, and compared to other variables. In addition, a set of climate change indicators (Table 2) is calculated from the results. All 27 climatic, hydrological, and drought signatures can be assessed in a `Dash` board of customizable figures. Finally, two static figures that summarize the ensemble projections of key variables through the 21st century are generated (see Schuster et al. 2025d).

4 Sensitivity analysis

Due to MATILDA's many interrelated parameters, sensitivity analysis is essential to reduce the parameter space and support users with limited computational resources. Global sensitivity was evaluated using five runs of the extended Fourier Amplitude Sensitivity Test (FAST) by A. Saltelli and Chan (1999). All parameters were sampled from uniform distributions within default bounds (Table1) over 1,500,012 iterations. **(1)** The first run included all 21 parameters. **(2)** Then, three HBV parameters correcting input errors were excluded to isolate internal model sensitivities: The correction factors for snowfall (SFCF)

https://doi.org/10.5194/egusphere-2025-3461
Preprint. Discussion started: 15 December 2025

and evaporation (CET) were disabled fixing them at 1 and 0, respectively. The precipitation correction factor (PCORR) was calibrated using the posterior mean of stratified random samples of all water balance related parameters (see Schuster et al. 2025d). Finally, **(3-5)** the FAST was repeated for three glacier cover scenarios. The glacierized fraction of the example catchment (10.8 %) was varied to 50 %, 30 % and 0 %, respectively, by linearly adjusting the glacier profile while maintaining elevation distribution.

Figure 3 illustrates parameter sensitivity with and without input correction factors, and for different glacier cover fractions. The HBV model shows extreme sensitivity to input correction factors, especially those related to precipitation, which tend to mask internal sensitivities. The snow melt factor ($CFMAX_{snow}$) has a significant effect on runoff in every configuration and is the dominant parameter at high glacier cover. The upper groundwater box recession coefficient (K_1) stands out as the dominant parameter in the ice-free catchment, but its significance diminishes when glacier cover exceeds 10%. Soil parameters such as field capacity (FC) and shape coefficient (BETA), as well as the threshold for groundwater runoff (UZL), become more important with lower glacier cover. Conversely, lapse rates (lr_{temp}, lr_{prec}), the refreezing coefficient (CFR), at least one threshold temperature (TT_{snow}/TT_{diff}), soil evaporation reduction (LP), and the routing parameter (MAXBAS) are below the sensitivity threshold of 0.05 in all experiments. Using this threshold, the number of low-sensitivity parameters varies by glacier cover: 10 (for 0 % glacier cover), 6 (10.8 %), 12 (30 %), and 15 (50 %), allowing for substantial reduction in calibration time with minimal performance loss, depending in the initial catchment conditions.

5 Limitations

5.1 Spatial Aggregation

As a lumped model, MATILDA does not capture spatial variability from terrain shading, elevation-dependent warming, or orographic effects. This impairs the accurate representation of snowmelt and consequently the timing of runoff. Additionally, glaciers in favorable topography may persist longer. While semi-distributed models can improve runoff timing (Khakbaz et al., 2012; Shannon et al., 2023), especially in nival basins (Garavaglia et al., 2017), hydrological research units or additional subcatchments increase computational demands, calibration complexity, and reduce accessibility. Without appropriate data to constrain the model, added complexity does not improve runoff simulation (Finger et al., 2015). Thus, data availability outweighs model structure.

5.2 Sublimation

MATILDA simplifies snow and glacier processes, notably by omitting explicit snow sublimation, a key factor in glacio-hydrological modeling (Strasser et al., 2008; Gascoin et al., 2013; Stigter et al., 2018; Sauter et al., 2020). Sublimation reduces both energy for snowmelt (Hock, 2003) and the amount of snow considered as melt runoff, and can account for up to 90 % of total ablation in arid, wind-exposed regions (Strasser et al., 2008). High sublimation leads to low degree-day factors due to its high energy consumption (Hock, 2003). While physical estimation is possible using wind and humidity, HBV typically

https://doi.org/10.5194/egusphere-2025-3461
Preprint. Discussion started: 15 December 2025

addresses sublimation via the snowfall correction factor (SFCF). In this study, SFCF was fixed to isolate internal sensitivities and because sublimation is already addressed in the snow reanalysis (Liu et al., 2021b) used for model calibration (Schuster et al., 2025d).

5.3 Glacial Modeling

The Δh routine by Seibert et al. (2018) assumes clean-ice valley glaciers with parabolic geometry. However, debris cover alters melt rates—enhancing them when thin and reducing them for higher thicknesses (Shukla and Qadir, 2016; Anderson et al., 2018). A debris-enhanced model by Carenzo et al. (2016) addresses this but adds six parameters and requires shortwave radiation and debris data. Though Rounce et al. (2021) provide debris estimates for all RGI6 glaciers, catchment-wide aggregates have high uncertainty without consideration of glacier dynamics. Thick debris may reduce ablation and promote permafrost features like rock glaciers (Anderson et al., 2018; Jones et al., 2019), which are not modeled in MATILDA but could influence future runoff as shallow aquifers providing retarded runoff during dry periods (Wagner et al., 2021).

MATILDA's modular design allows replacing the glacier routine with a more comprehensive glacier model (e.g., OGGM; Maussion et al. 2019) to account glacier dynamics and spatial variability. Nevertheless, the uncertainties propagated by the calibration data remain regardless of the modeling approach (Schuster et al., 2025d) and become more important with higher glacier cover (Shannon et al., 2023).

6 Conclusions

MATILDA offers a broad user base easy access, simplicity, and low technical requirements. Its modular design and availability as a Python package enhance its usability and adaptability. Leveraging open data and cloud services enables streamlined hydrological modeling across regions and use cases. MATILDA's simplistic design is particularly useful for studies requiring large sample sizes. Its Jupyter Book format, paired with an online Python environment, integrates comprehensive documentation with practical execution. However, as discussed in the follow-up study (Schuster et al., 2025d), these benefits come with significant uncertainties.

Despite its accessibility, effective calibration and interpretation still require expert knowledge (Photiadou et al., 2021). Open-source services like MATILDA help address this obstacle by promoting reproducibility, collaboration, and communication (Gan et al., 2020; Gichamo et al., 2020). The model, tools, and example data are freely available to facilitate community engagement. Stakeholder participation, shared knowledge, and accessible tools for monitoring and projecting future conditions are essential for integrated water management in the context of climate change (IPCC, 2019). Tools like MATILDA can inform, educate, and empower stakeholders in water resource management and science in vulnerable regions, enhancing the effectiveness of water management strategies in the face of the challenges ahead.

Part two of this study applies MATILDA to a case study, evaluates performance and uncertainties, and and discusses potential improvements (Schuster et al., 2025d). Future releases aim to expand the tool through community contributions and broader regional applications.

https://doi.org/10.5194/egusphere-2025-3461
Preprint. Discussion started: 15 December 2025

Code availability. This paper refers to the v1.0.2 of the MATILDA Python package (Schuster et al., 2025c), which is accessible on Zenodo via https://doi.org/10.5281/zenodo.16049093, and v1.0.1 of the online workflow MATILDA-Online (Schuster et al., 2025a), accessible via https://doi.org/10.5281/zenodo.16059509. The source code and related resources, such as example datasets, repositories, and manuals are available there. Both the core model and the online workflow are distributed under the MIT license. Additionally, the latest version of MATILDA-Online is deployed as a Jupyter Book at https://matilda-online.github.io/jbook (Schuster et al., 2025b). Each Notebook can be executed locally or in an online Python environment hosted on mybinder.org (Project Jupyter et al., 2018).

The tool has cross-platform compatibility and was developed on Ubuntu 22.04.4 LTS and Windows 11. It can be executed on any operating system supporting Python 3.11 and Jupyter Notebook. For optimal calibration performance, parallel processing is recommended, which may require further dependencies. The calibration module was specifically developed and tested on a desktop computer running Ubuntu 22.04.4 LTS and an HPC system running Rocky Linux 8.6. Detailed installation guidelines, dependencies, and usage examples are provided in the repositories and the website referenced above.

Competing interests. The authors declare that the research was conducted in the absence of any commercial or financial relationships that could be construed as a potential conflict of interest.

Author contributions. C. Schneider and P. Schuster were responsible for funding acquisition and the principal conceptualization of the approach in this study. P. Schuster and A. Tappe developed the Python package containing the core modeling routines. A. Georgi, P. Schuster, and Mia Janzen developed the MATILDA-Online workflow and the website. Processing steps and results were discussed among all authors. P. Schuster prepared the publication including text and figures. C. Schneider and T. Sauter supervised the work and assisted in editing the final paper.

Acknowledgements. The first pre-release version of the matilda Python package was developed within the frame of the project 'Ecosystem-based Adaptation in High Mountainous Regions of Central Asia' (https://www.giz.de/en/worldwide/40944.html) funded by the Deutsche Gesellschaft für Internationale Zusammenarbeit (GIZ) GmbH. Further work was funded by the Humboldt-Universität zu Berlin. The authors would like to thank the colleagues at the Central Asian Institute of Applied Geosciences in Bishkek, Kyrgyzstan, who provided valuable support during fieldwork and workshops, as well as data and insightful feedback. We also thank the Kyrgyz Hydrometeorological Service (Kyrgyz Hydromet) for providing runoff data. We thank our partners at the GIZ office in Bishkek for their assistance with international affairs and for hosting the MATILDA workshops. We also thank Marc Vis for his assistance in adapting the Δh glacier parameterization in Python, Daniel Farinotti for his immediate assistance with the ice thickness dataset, and Christopher Schneider and Larissa Lachmann for their exceptional guidance in graphic design.

The following AI tools were used for preparing this manuscript: Consensus.app (https://consensus.app) for literature research, NotebookLM by Google (https://notebooklm.google) for literature summaries, DeepL Write (https://www.deepl.com/write) and ChatGPT 4o (https://openai.com/chatgpt) for grammar and spelling checks, and text shortening, ChatGPT 4o for LaTeX and figure editing, and Midjourney (https://www.midjourney.com) for the original draft of the "cupcake" figure.

https://doi.org/10.5194/egusphere-2025-3461
Preprint. Discussion started: 15 December 2025

References

Google Earth Engine API, https://developers.google.com/earth-engine/apidocs, accessed: 2025-01-27, 2025.

A. Saltelli, S. T. and Chan, K. P.-S.: A Quantitative Model-Independent Method for Global Sensitivity Analysis of Model Output, Technometrics, 41, 39–56, https://doi.org/10.1080/00401706.1999.10485594, 1999.

Aggarwal, A., Frey, H., McDowell, G., Drenkhan, F., Nüsser, M., Racoviteanu, A., and Hoelzle, M.: Adaptation to climate change induced water stress in major glacierized mountain regions, Climate and Development, 14, 665–677, https://doi.org/10.1080/17565529.2021.1971059, 2022.

Alcantara, M. A. S., Nelson, E. J., Shakya, K., Edwards, C., Roberts, W. R., Krewson, C., Ames, D. P., Jones, N., and Gutierrez, A.: Hydrologic Modeling as a Service (HMaaS): A New Approach to Address Hydroinformatic Challenges in Developing Countries, Frontiers in Environmental Science, https://doi.org/10.3389/fenvs.2019.00158, 2019.

Alfieri, L., Burek, P., Dutra, E., Krzeminski, B., Muraro, D., Thielen, J., and Pappenberger, F.: GloFAS ndash; global ensemble streamflow forecasting and flood early warning, Hydrology and Earth System Sciences, 17, 1161–1175, https://doi.org/10.5194/hess-17-1161-2013, 2013.

Ali, A., Dunlop, P., Coleman, S., Kerr, D., McNabb, R., and Noormets, R.: Glacier area changes in Novaya Zemlya from 1986–89 to 2019–21 using object-based image analysis in Google Earth Engine, Journal of Glaciology, 69, 1–12, https://doi.org/10.1017/jog.2023.18, 2023.

Allan, R., Pereira, L., and Smith, M.: Crop evapotranspiration-Guidelines for computing crop water requirements-FAO Irrigation and drainage paper 56, 56, 1–15, 1998.

Anderson, R., Anderson, L., Armstrong, W., Rossi, M., and Crump, S.: Glaciation of alpine valleys: The glacier – debris-covered glacier – rock glacier continuum, Geomorphology, https://doi.org/10.1016/J.GEOMORPH.2018.03.015, 2018.

Arheimer, B., Pimentel, R., Isberg, K., Crochemore, L., Andersson, J. C. M., Hasan, A., and Pineda, L.: Global catchment modelling using World-Wide HYPE (WWH), open data, and stepwise parameter estimation, Hydrology and Earth System Sciences, 24, 535–559, https://doi.org/10.5194/hess-24-535-2020, 2020.

Arsenault, R., Brissette, F., and Martel, J.-L.: The hazards of split-sample validation in hydrological model calibration, Journal of Hydrology, 566, 346–362, https://doi.org/https://doi.org/10.1016/j.jhydrol.2018.09.027, 2018.

Ayzel, G.: LHMP: First major release, https://doi.org/10.5281/zenodo.59680, 2016.

Barandun, M., Pohl, E., Naegeli, K., McNabb, R., Huss, M., Berthier, E., Saks, T., and Hoelzle, M.: Hot Spots of Glacier Mass Balance Variability in Central Asia, Geophysical Research Letters, 48, e2020GL092 084, https://doi.org/https://doi.org/10.1029/2020GL092084, e2020GL092084 2020GL092084, 2021.

Bartos, M.: pysheds: simple and fast watershed delineation in python, https://doi.org/10.5281/zenodo.3822494, 2020.

Bergström, S.: Development and Application of a Conceptual Runoff Model for Scandinavian Catchments, vol. 134 pp., 1976.

Bergström, S. and Lindström, G.: Interpretation of runoff processes in hydrological modelling—experience from the HBV approach, Hydrological Processes, 29, 3535–3545, https://doi.org/https://doi.org/10.1002/hyp.10510, 2015.

Beven, K. and Binley, A.: The future of distributed models: Model calibration and uncertainty prediction, Hydrological Processes, 6, 279–298, https://doi.org/10.1002/hyp.3360060305, 1992.

Birhanu, D., Kim, H., Jang, C., and Park, S.: Does the Complexity of Evapotranspiration and Hydrological Models Enhance Robustness?, Sustainability, 10, https://doi.org/10.3390/su10082837, 2018.

https://doi.org/10.5194/egusphere-2025-3461
Preprint. Discussion started: 15 December 2025

Biswas, N. and Hossain, F.: A scalable open-source Web-analytic framework to improve satellite-based operational water management in developing countries, Journal of Hydroinformatics, 20, 49–68, https://doi.org/10.2166/HYDRO.2017.073, 2018.

Brooking, C. and Hunter, J.: Providing online access to hydrological model simulations through interactive geospatial animations, Environmental Modelling Software, 43, 163–168, https://doi.org/10.1016/j.envsoft.2013.01.011, 2013.

Carenzo, M., Pellicciotti, F., Mabillard, J., Reid, T., and Brock, B.: An enhanced temperature index model for debris-covered glaciers accounting for thickness effect, Advances in Water Resources, 94, 457–469, https://doi.org/https://doi.org/10.1016/j.advwatres.2016.05.001, 2016.

Chen, Y., Li, Z., Fang, G., and Li, W.: Large Hydrological Processes Changes in the Transboundary Rivers of Central Asia, Journal of Geophysical Research: Atmospheres, 123, 5059–5069, https://doi.org/https://doi.org/10.1029/2017JD028184, 2018.

Clark, M. P., Kavetski, D., and Fenicia, F.: Pursuing the method of multiple working hypotheses for hydrological modeling, Water Resources Research, 47, https://doi.org/https://doi.org/10.1029/2010WR009827, 2011.

Compagno, L., Zekollari, H., Huss, M., and Farinotti, D.: Limited Impact of Climate Forcing Products on Future Glacier Evolution in Scandinavia and Iceland, Journal of Glaciology, https://doi.org/10.1017/jog.2021.24, 2021.

De Filippis, T., Rocchi, L., Massazza, G., Pezzoli, A., Rosso, M., Housseini Ibrahim, M., and Tarchiani, V.: Hydrological Web Services for Operational Flood Risk Monitoring and Forecasting at Local Scale in Niger, ISPRS International Journal of Geo-Information, 11, https://doi.org/10.3390/ijgi11040236, 2022.

Donnelly, C., Andersson, J. C., and Arheimer, B.: Using flow signatures and catchment similarities to evaluate the E-HYPE multi-basin model across Europe, Hydrological Sciences Journal, 61, 255–273, https://doi.org/10.1080/02626667.2015.1027710, 2016.

Duethmann, D., Peters, J., Blume, T., Vorogushyn, S., and Güntner, A.: The value of satellite-derived snow cover images for calibrating a hydrological model in snow-dominated catchments in Central Asia, Water Resources Research, 50, 2002–2021, https://doi.org/10.1002/2013WR014382, 2014.

Duethmann, D., Bolch, T., Farinotti, D., Kriegel, D., Vorogushyn, S., Merz, B., Pieczonka, T., Jiang, T., Su, B., and Güntner, A.: Attribution of streamflow trends in snow and glacier melt-dominated catchments of the Tarim River, Central Asia, Water Resources Research, 51, 4727–4750, https://doi.org/https://doi.org/10.1002/2014WR016716, 2015.

Erazo Ramirez, C., Sermet, Y., Molkenthin, F., and Demir, I.: HydroLang: An open-source web-based programming framework for hydrological sciences, Environmental Modelling Software, 157, 105 525, https://doi.org/https://doi.org/10.1016/j.envsoft.2022.105525, 2022.

Ewing, G., Mantilla, R., Krajewski, W., and Demir, I.: Interactive hydrological modelling and simulation on client-side web systems: an educational case study, Journal of Hydroinformatics, 24, 1194–1206, https://doi.org/10.2166/hydro.2022.061, 2022.

Eyring, V., Bony, S., Meehl, G. A., Senior, C. A., Stevens, B., Stouffer, R. J., and Taylor, K. E.: Overview of the Coupled Model Intercomparison Project Phase 6 (CMIP6) Experimental Design and Organization, Geoscientific Model Development, 9, 1937–1958, https://doi.org/10.5194/gmd-9-1937-2016, 2016.

Farinotti, D., Huss, M., Fürst, J. J., Landmann, J. M., Machguth, H., Maussion, F., and Pandit, A.: A consensus estimate for the ice thickness distribution of all glaciers on Earth, Nature Geoscience, 12, 168–173, https://api.semanticscholar.org/CorpusID:134718890, 2019.

Finger, D., Vis, M., Huss, M., and Seibert, J.: The value of multiple data set calibration versus model complexity for improving the performance of hydrological models in mountain catchments, Water Resources Research, 51, 1939–1958, https://doi.org/https://doi.org/10.1002/2014WR015712, 2015.

https://doi.org/10.5194/egusphere-2025-3461
Preprint. Discussion started: 15 December 2025

Gan, T., Tarboton, D. G., Dash, P., Gichamo, T., and Horsburgh, J. S.: Integrating Hydrologic Modeling Web Services With Online Data Sharing to Prepare, Store, and Execute Hydrologic Models, Environmental Modelling & Software, https://doi.org/10.1016/j.envsoft.2020.104731, 2020.

Garavaglia, F., Le Lay, M., Gottardi, F., Garçon, R., Gailhard, J., Paquet, E., and Mathevet, T.: Impact of model structure on flow simulation and hydrological realism: from a lumped to a semi-distributed approach, Hydrology and Earth System Sciences, 21, 3937–3952, https://doi.org/10.5194/hess-21-3937-2017, 2017.

Gascoin, S., Lhermitte, S., Kinnard, C., Bortels, K., and Liston, G. E.: Wind effects on snow cover in Pascua-Lama, Dry Andes of Chile, Advances in Water Resources, 55, 25–39, https://doi.org/https://doi.org/10.1016/j.advwatres.2012.11.013, snow–Atmosphere Interactions and Hydrological Consequences, 2013.

Gholami, H., Lotfirad, M., Ashrafi, S. M., Biazar, S. M., and Singh, V. P.: Multi-GCM ensemble model for reduction of uncertainty in runoff projections, Stochastic Environmental Research and Risk Assessment, 37, 953–964, https://doi.org/10.1007/s00477-022-02311-1, 2023.

Gichamo, T. Z., Sazib, N. S., Tarboton, D. G., and Dash, P.: HydroDS: Data services in support of physically based, distributed hydrological models, Environmental Modelling Software, 125, 104 623, https://doi.org/https://doi.org/10.1016/j.envsoft.2020.104623, 2020.

Gorelick, N., Hancher, M., Dixon, M., Ilyushchenko, S., Thau, D., and Moore, R.: Google Earth Engine: Planetary-scale geospatial analysis for everyone, Remote Sensing of Environment, 202, 18–27, https://doi.org/https://doi.org/10.1016/j.rse.2017.06.031, big Remotely Sensed Data: tools, applications and experiences, 2017.

Guo, D., Zheng, F., Gupta, H., and Maier, H. R.: On the Robustness of Conceptual Rainfall-Runoff Models to Calibration and Evaluation Data Set Splits Selection: A Large Sample Investigation, Water Resources Research, 56, e2019WR026 752, https://doi.org/https://doi.org/10.1029/2019WR026752, e2019WR026752 2019WR026752, 2020.

Hagg, W., Braun, L., Kuhn, M., and Nesgaard, T.: Modelling of hydrological response to climate change in glacierized Central Asian catchments, Journal of Hydrology, 332, 40–53, https://doi.org/https://doi.org/10.1016/j.jhydrol.2006.06.021, 2007.

Her, Y. and Chaubey, I.: Impact of the numbers of observations and calibration parameters on equifinality, model performance, and output and parameter uncertainty, Hydrological Processes, 29, 4220–4237, https://doi.org/10.1002/hyp.10487, 2015.

Her, Y. and Seong, C.: Responses of hydrological model equifinality, uncertainty, and performance to multi-objective parameter calibration, Journal of Hydroinformatics, 20, 864–885, https://doi.org/10.2166/hydro.2018.108, 2018.

Hock, R.: Temperature index melt modelling in mountain areas, Journal of Hydrology, 282, 104–115, https://doi.org/https://doi.org/10.1016/S0022-1694(03)00257-9, mountain Hydrology and Water Resources, 2003.

Hock, R., Rasul, G., Adler, C., Caceres, B., Gruber, S., Hirabayashi, Y., Jackson, M., Kääb, A., Kang, S., Kutuzov, S., Milner, A., Molau, U., Morin, S., Orlove, B., Steltzer, H., Allen, S., Arenson, L., Baneerjee, S., Barr, I., Bórquez, R., Brown, L., Cao, B., Carey, M., Cogley, G., Fischlin, A., de Sherbinin, A., Eckert, N., Geertsema, M., Hagenstad, M., Honsberg, M., Hood, E., Huss, M., Zamora, E. J., Kotlarski, S., Lefeuvre, P., Moreno, J. I. L., Lundquist, J., McDowell, G., Mills, S., Mou, C., Nepal, S., Noetzli, J., E, P., Pepin, N., Rixen, C., Shahgedanova, M., Skiles, S. M., Vincent, C., Viviroli, D., Weyhenmeyer, G. A., Sherpa, P. Y., Weyer, N., Wouters, B., Yasunari, T., You, Q., and Zhang, Y.: High Mountain Areas, in: The Ocean and Cryosphere in a Changing Climate: Special Report of the Intergovernmental Panel on Climate Change, edited by Pörtner, H.-O., Roberts, D., Masson-Delmotte, V., Zhai, P., Tignor, M., Poloczanska, E., Mintenbeck, K., Alegría, A., Nicolai, M., Okem, A., Petzold, J., Rama, B., and Weyer, N., p. 131–202, Cambridge University Press, Cambridge, UK and New York, NY, USA, https://doi.org/10.1017/9781009157964.004, 2019.

Holdgraf, C., Kleinert, J., DuPre, E., Jas, M., Morley, A., Brett, M., Craig, M., Sundell, E., Lau, S., Luke, gaow, stafforddavidj, cnydw, Sailer, Z., Tom, Boudreau, M., Mason, J., and Rokem, A.: jupyter/jupyter-book: v0.5, https://doi.org/10.5281/zenodo.2799972, 2019.

https://doi.org/10.5194/egusphere-2025-3461
Preprint. Discussion started: 15 December 2025

Horton, P., Schaefli, B., and Kauzlaric, M.: Why do we have so many different hydrological models? A review based on the case of Switzerland, WIREs Water, 9, e1574, https://doi.org/https://doi.org/10.1002/wat2.1574, 2022.

Houska, T., Kraft, P., Chamorro-Chavez, A., and Breuer, L.: SPOTting Model Parameters Using a Ready-Made Python Package, PLOS ONE, 10, 1–22, https://doi.org/10.1371/journal.pone.0145180, 2015.

Huss, M. and Fischer, M.: Sensitivity of Very Small Glaciers in the Swiss Alps to Future Climate Change, Frontiers in Earth Science, 4, https://doi.org/10.3389/feart.2016.00034, 2016.

Huss, M., Jouvet, G., Farinotti, D., and Bauder, A.: Future high-mountain hydrology: a new parameterization of glacier retreat, Hydrology and Earth System Sciences, 14, 815–829, https://doi.org/10.5194/hess-14-815-2010, 2010.

Immerzeel, W. W., Lutz, A. F., Andrade, M., Bahl, A., Biemans, H., Bolch, T., Hyde, S., Brumby, S., Davies, B., Elmore, A., et al.: Importance and vulnerability of the world's water towers, Nature, 577, 364–369, 2020.

Jadidoleslam, N., Goska, R., Mantilla, R., and Krajewski, W. F.: Hydrovise: A non-proprietary open-source software for hydrologic model and data visualization and evaluation, Environmental Modelling Software, 134, 104 853, https://doi.org/https://doi.org/10.1016/j.envsoft.2020.104853, 2020.

Jones, D. B., Harrison, S., and Anderson, K.: Mountain glacier-to-rock glacier transition, Global and Planetary Change, https://doi.org/10.1016/J.GLOPLACHA.2019.102999, 2019.

Khakbaz, B., Imam, B., Hsu, K., and Sorooshian, S.: From lumped to distributed via semi-distributed: Calibration strategies for semi-distributed hydrologic models, Journal of Hydrology, 418-419, 61–77, https://doi.org/10.1016/j.jhydrol.2009.02.021, the Distributed Model Intercomparison Project (DMIP) - Phase 2 Experiments in the Oklahoma Region, USA, 2012.

Kim, J. and Ryu, J. H.: Quantifying the Performances of the Semi-Distributed Hydrologic Model in Parallel Computing—A Case Study, Water, 11, https://doi.org/10.3390/w11040823, 2019.

Klemeš, V.: Operational testing of hydrological simulation models, Hydrological Sciences Journal, 31, 13–24, https://doi.org/10.1080/02626668609491024, 1986.

Kuczera, G. and Mroczkowski, M.: Assessment of hydrologic parameter uncertainty and the worth of multiresponse data, Water Resources Research, 34, 1481–1489, https://doi.org/10.1029/98WR00496, 1998.

Kumar, P.: bias_correction: Python library for bias correction, https://github.com/pankajkarman/bias_correction, 2022.

Lew, R., Dobre, M., Srivastava, A., Brooks, E. S., Elliot, W. J., Robichaud, P. R., and Flanagan, D. C.: WEPP-cloud: An online watershed-scale hydrologic modeling tool. Part I. Model description, Journal of Hydrology, 608, 127 603, https://doi.org/https://doi.org/10.1016/j.jhydrol.2022.127603, 2022.

Lindström, G. and Bergström, S.: Improving the HBV and PULSE-models by use of temperature anomalies, Vannet i Norden, 1, 16–23, 1992.

Liu, Y., Fang, Y., and Margulis, S. A.: High Mountain Asia UCLA Daily Snow Reanalysis, Version 1, https://doi.org/10.5067/HNAUGJQXSCVU, 2021a.

Liu, Y., Fang, Y., and Margulis, S. A.: Spatiotemporal distribution of seasonal snow water equivalent in High Mountain Asia from an 18-year Landsat–MODIS era snow reanalysis dataset, The Cryosphere, 15, 5261–5280, https://doi.org/10.5194/tc-15-5261-2021, 2021b.

Margulis, S. A., Liu, Y., and Baldo, E.: A Joint Landsat- and MODIS-Based Reanalysis Approach for Midlatitude Montane Seasonal Snow Characterization, Frontiers in Earth Science, 7, https://doi.org/10.3389/feart.2019.00272, 2019.

https://doi.org/10.5194/egusphere-2025-3461
Preprint. Discussion started: 15 December 2025

Maussion, F., Butenko, A., Champollion, N., Dusch, M., Eis, J., Fourteau, K., Gregor, P., Jarosch, A. H., Landmann, J., Oesterle, F., Recinos, B., Rothenpieler, T., Vlug, A., Wild, C. T., and Marzeion, B.: The Open Global Glacier Model (OGGM) v1.1, Geoscientific Model Development, 12, 909–931, https://doi.org/10.5194/gmd-12-909-2019, 2019.

McDonald, S., Mohammed, I. N., Bolten, J. D., Pulla, S., Meechaiya, C., Markert, A., Nelson, E. J., Srinivasan, R., and Lakshmi, V.: Web-based decision support system tools: The Soil and Water Assessment Tool Online visualization and analyses (SWATOnline) and NASA earth observation data downloading and reformatting tool (NASAaccess), Environmental Modelling Software, 120, 104 499, https://doi.org/https://doi.org/10.1016/j.envsoft.2019.104499, 2019.

Miles, E. S., McCarthy, M., Dehecq, A., Kneib, M., Fugger, S., and Pellicciotti, F.: Health and Sustainability of Glaciers in High Mountain Asia, Nature Communications, https://doi.org/10.1038/s41467-021-23073-4, 2021.

Monteith, J. L.: Evaporation and environment., Symposia of the Society for Experimental Biology, 19, 205–34, 1965.

Muñoz Sabater, J., Dutra, E., Agustí-Panareda, A., Albergel, C., Arduini, G., Balsamo, G., Boussetta, S., Choulga, M., Harrigan, S., Hersbach, H., Martens, B., Miralles, D. G., Piles, M., Rodríguez-Fernández, N. J., Zsoter, E., Buontempo, C., and Thépaut, J.-N.: ERA5-Land: a state-of-the-art global reanalysis dataset for land applications, Earth System Science Data, 13, 4349–4383, https://doi.org/10.5194/essd-13-4349-2021, 2021.

Nemri, S. and Kinnard, C.: Comparing calibration strategies of a conceptual snow hydrology model and their impact on model performance and parameter identifiability, Journal of Hydrology, 582, 124 474, https://doi.org/10.1016/j.jhydrol.2019.124474, 2020.

Oudin, L., Hervieu, F., Michel, C., Perrin, C., Andréassian, V., Anctil, F., and Loumagne, C.: Which potential evapotranspiration input for a lumped rainfall–runoff model?: Part 2—Towards a simple and efficient potential evapotranspiration model for rainfall–runoff modelling, Journal of Hydrology, 303, 290–306, https://doi.org/https://doi.org/10.1016/j.jhydrol.2004.08.026, 2005.

Ougahi, J. H. and Mahmood, S. A.: Evaluation of satellite-based and reanalysis precipitation datasets by hydrologic simulation in the Chenab river basin, Journal of Water and Climate Change, 13, 1563–1582, https://doi.org/10.2166/wcc.2022.410, 2022.

Paul, P. K., Zhang, Y., Ma, N., Mishra, A., Panigrahy, N., and Singh, R.: Selecting hydrological models for developing countries: Perspective of global, continental, and country scale models over catchment scale models, Journal of Hydrology, 600, 126 561, https://doi.org/https://doi.org/10.1016/j.jhydrol.2021.126561, 2021.

Photiadou, C., Arheimer, B., Bosshard, T., Capell, R., Elenius, M., Gallo, I., Gyllensvärd, F., Klehmet, K., Little, L., Ribeiro, I., Santos, L., and Sjökvist, E.: Designing a Climate Service for Planning Climate Actions in Vulnerable Countries, Atmosphere, 12, https://doi.org/10.3390/atmos12010121, 2021.

Plotly Technologies Inc.: Collaborative data science, https://plot.ly, 2015.

Pohl, E., Gloaguen, R., Andermann, C., and Knoche, M.: Glacier melt buffers river runoff in the P amir M ountains, Water Resources Research, 53, 2467–2489, 2017.

Pritchard, H. D.: Asia's shrinking glaciers protect large populations from drought stress, Nature, 569, 649–654, 2019.

Probst, E. and Mauser, W.: Evaluation of ERA5 and WFDE5 forcing data for hydrological modelling and the impact of bias correction with regional climatologies: A case study in the Danube River Basin, Journal of Hydrology: Regional Studies, 40, 101 023, https://doi.org/https://doi.org/10.1016/j.ejrh.2022.101023, 2022.

Project Jupyter, Matthias Bussonnier, Jessica Forde, Jeremy Freeman, Brian Granger, Tim Head, Chris Holdgraf, Kyle Kelley, Gladys Nalvarte, Andrew Osheroff, Pacer, M., Yuvi Panda, Fernando Perez, Benjamin Ragan Kelley, and Carol Willing: Binder 2.0 - Reproducible, interactive, sharable environments for science at scale, in: Proceedings of the 17th Python in Science Conference, edited by Fatih Akici, David Lippa, Dillon Niederhut, and Pacer, M., pp. 113 – 120, https://doi.org/10.25080/Majora-4af1f417-011, 2018.

https://doi.org/10.5194/egusphere-2025-3461
Preprint. Discussion started: 15 December 2025

Rajib, A., Kim, I. L., Ercan, M. B., Merwade, V., Zhao, L., Song, C., and Lin, K.-H.: Cyber-enabled autocalibration of hydrologic models to support Open Science, Environmental Modelling Software, 158, 105 561, https://doi.org/https://doi.org/10.1016/j.envsoft.2022.105561, 2022.

RGI Consortium: Randolph Glacier Inventory - A Dataset of Global Glacier Outlines, Version 6, Boulder, Colorado USA. NSIDC: National Snow and Ice Data Center, https://doi.org/https://doi.org/10.7265/4m1f-gd79, 2017.

Rounce, D. R., Hock, R., and Shean, D.: Glacier Mass Change in High Mountain Asia Through 2100 Using the Open-Source Python Glacier Evolution Model (PyGEM), Frontiers in Earth Science, https://doi.org/10.3389/feart.2019.00331, 2020.

Rounce, D. R., Hock, R., McNabb, R. W., Millan, R., Sommer, C., Braun, M. H., Malz, P., Maussion, F., Mouginot, J., Seehaus, T. C., and Shean, D. E.: Distributed Global Debris Thickness Estimates Reveal Debris Significantly Impacts Glacier Mass Balance, Geophysical Research Letters, 48, e2020GL091 311, https://doi.org/https://doi.org/10.1029/2020GL091311, e2020GL091311 2020GL091311, 2021.

Sanchez Lozano, J., Romero Bustamante, G., Hales, R. C., Nelson, E. J., Williams, G. P., Ames, D. P., and Jones, N. L.: A Streamflow Bias Correction and Performance Evaluation Web Application for GEOGloWS ECMWF Streamflow Services, Hydrology, 8, https://doi.org/10.3390/hydrology8020071, 2021.

Sauter, T., Arndt, A., and Schneider, C.: COSIPY v1.3 – an open-source coupled snowpack and ice surface energy and mass balance model, Geoscientific Model Development, 13, 5645–5662, https://doi.org/10.5194/gmd-13-5645-2020, 2020.

Schaffhauser, T., Lange, S., Tuo, Y., and Disse, M.: Shifted discharge and drier soils: Hydrological projections for a Central Asian catchment, Journal of Hydrology: Regional Studies, 46, 101 338, https://doi.org/https://doi.org/10.1016/j.ejrh.2023.101338, 2023.

Schuster, P., Georgi, A., and Janzen, M.: MATILDA-Online: Cloud-based Workflow for Modeling wATer resources In gLacierizeD cAtchments, https://doi.org/10.5281/zenodo.16059509, 2025a.

Schuster, P., Georgi, A., and Janzen, M.: MATILDA-Online: Cloud-based Workflow for Modeling wATer resources In gLacierizeD cAtchments - Jupyter Book, https://matilda-online.github.io/jbook, 2025b.

Schuster, P., Georgi, A., and Tappe, A.-L.: MATILDA: Modeling wATer resources In gLacierizeD cAtchments, https://doi.org/10.5281/zenodo.16049093, 2025c.

Schuster, P., Osmonov, A., Tappe, A.-L., Georgi, A., Schneider, C., and Sauter, T.: Climate Impacts on Water Resources in a High Mountain Catchment: Application of the Open-Source Modeling Workflow MATILDA in the Northern Tian Shan, Hydrology and Earth System Sciences, manuscript submitted for publication, 2025d.

Seguinot, J.: PyPDD: a positive degree day model for glacier surface mass balance, https://doi.org/10.5281/zenodo.3467639, 2019.

Seibert, J. and Vis, M. J. P.: Teaching hydrological modeling with a user-friendly catchment-runoff-model software package, Hydrology and Earth System Sciences, 16, 3315–3325, https://doi.org/10.5194/hess-16-3315-2012, 2012.

Seibert, J., Vis, M. J. P., Kohn, I., Weiler, M., and Stahl, K.: Technical note: Representing glacier geometry changes in a semi-distributed hydrological model, Hydrology and Earth System Sciences, 22, 2211–2224, https://doi.org/10.5194/hess-22-2211-2018, 2018.

Shannon, S., Payne, A., Freer, J., Coxon, G., Kauzlaric, M., Kriegel, D., and Harrison, S.: A snow and glacier hydrological model for large catchments – case study for the Naryn River, central Asia, Hydrology and Earth System Sciences, 27, 453–480, https://doi.org/10.5194/hess-27-453-2023, 2023.

Shean, D. E., Bhushan, S., Montesano, P., Rounce, D. R., Arendt, A., and Osmanoglu, B.: A Systematic, Regional Assessment of High Mountain Asia Glacier Mass Balance, Frontiers in Earth Science, 7, https://doi.org/10.3389/feart.2019.00363, 2020.

Shen, H., Tolson, B. A., and Mai, J.: Time to Update the Split-Sample Approach in Hydrological Model Calibration, Water Resources Research, 58, e2021WR031 523, https://doi.org/https://doi.org/10.1029/2021WR031523, e2021WR031523 2021WR031523, 2022.

https://doi.org/10.5194/egusphere-2025-3461
Preprint. Discussion started: 15 December 2025

Shukla, A. and Qadir, J.: Differential response of glaciers with varying debris cover extent: evidence from changing glacier parameters, International Journal of Remote Sensing, 37, 2453–2479, https://doi.org/10.1080/01431161.2016.1176272, 2016.

Silvestro, F., Gabellani, S., Rudari, R., Delogu, F., Laiolo, P., and Boni, G.: Uncertainty reduction and parameter estimation of a distributed hydrological model with ground and remote-sensing data, Hydrology and Earth System Sciences, 19, 1727–1751, https://doi.org/10.5194/hess-19-1727-2015, 2015.

Stagge, J., Rosenberg, D., Abdallah, A., Akbar, H., Attallah, N. A., and James, R.: Assessing data availability and research reproducibility in hydrology and water resources, Scientific Data, 6, https://doi.org/10.1038/sdata.2019.30, 2019.

Stahl, K., Moore, R. D., Shea, J. M., Hutchinson, D., and Cannon, A. J.: Coupled modelling of glacier and streamflow response to future climate scenarios, Water Resources Research, 44, https://doi.org/https://doi.org/10.1029/2007WR005956, 2008.

Stigter, E. E., Litt, M., Steiner, J. F., Bonekamp, P. N. J., Shea, J. M., Bierkens, M. F. P., and Immerzeel, W. W.: The Importance of Snow Sublimation on a Himalayan Glacier, Frontiers in Earth Science, 6, https://doi.org/10.3389/feart.2018.00108, 2018.

Strasser, U., Bernhardt, M., Weber, M., Liston, G. E., and Mauser, W.: Is snow sublimation important in the alpine water balance?, The Cryosphere, 2, 53–66, https://doi.org/10.5194/tc-2-53-2008, 2008.

Switanek, M. B., Troch, P. A., Castro, C. L., Leuprecht, A., Chang, H.-I., Mukherjee, R., and Demaria, E. M. C.: Scaled distribution mapping: a bias correction method that preserves raw climate model projected changes, Hydrology and Earth System Sciences, 21, 2649–2666, https://doi.org/10.5194/hess-21-2649-2017, 2017.

Tarek, M., Brissette, F. P., and Arsenault, R.: Evaluation of the ERA5 reanalysis as a potential reference dataset for hydrological modelling over North America, Hydrology and Earth System Sciences, 24, 2527–2544, https://doi.org/10.5194/hess-24-2527-2020, 2020.

Taylor, P., Rahman, J., O'Sullivan, J., Podger, G., Rosello, C., Parashar, A., Sengupta, A., Perraud, J.-M., Pollino, C., and Coombe, M.: Basin futures, a novel cloud-based system for preliminary river basin modelling and planning, Environmental Modelling Software, 141, 105 049, https://doi.org/https://doi.org/10.1016/j.envsoft.2021.105049, 2021.

Thrasher, B., Wang, W., Michaelis, A., Melton, F., Lee, T., and Nemani, R.: NASA Global Daily Downscaled Projections, CMIP6, Scientific Data, 9, https://doi.org/10.1038/s41597-022-01393-4, 2022.

Toum, E., Ruiz, L., Villalba, R., Masiokas, M., and Pitte, P.: The HBV.IANIGLA Hydrological Model, The R Journal, 13, https://doi.org/10.32614/RJ-2021-059, 2021.

UNESCO: UNESCO Recommendation on Open Science, UNESCO, Place de Fontenoy 7, 75352 Paris 07 SP, France, https://unesdoc.unesco.org/ark:/48223/pf0000379949, sC-PCB-SPP/2021/OS/UROS, 2021.

Vishwanth, A.: The Role of Water as a Non Traditional Security Challenge, Artha - Journal of Social Sciences, https://doi.org/10.12724/ajss.51.7, 2019.

Viviroli, D., Kummu, M., Meybeck, M., Kallio, M., and Wada, Y.: Increasing dependence of lowland populations on mountain water resources, Nature Sustainability, 3, 917–928, 2020.

Wagner, T., Kainz, S., Krainer, K., and Winkler, G.: Storage-discharge characteristics of an active rock glacier catchment in the Innere Ölgrube, Austrian Alps, Hydrological Processes, 35, e14 210, https://doi.org/https://doi.org/10.1002/hyp.14210, 2021.

WEF, W. E. F.: Global Risks 2015, 10th Edition, World Economic Forum, https://www3.weforum.org/docs/WEF_Global_Risks_2015_Report15.pdf, rEF: 090115, 2015.

WEF, W. E. F.: Global Risks Report 2023, 18th Edition, World Economic Forum, https://www.weforum.org/reports/global-risks-report-2023/, iSBN-13: 978-2-940631-36-0, 2023.

https://doi.org/10.5194/egusphere-2025-3461
Preprint. Discussion started: 15 December 2025

Winsemius, H. C., Schaefli, B., Montanari, A., and Savenije, H. H. G.: On the calibration of hydrological models in ungauged basins: A framework for integrating hard and soft hydrological information, Water Resources Research, 45, https://doi.org/https://doi.org/10.1029/2009WR007706, 2009.

Wood, A. W., Maurer, E. P., Kumar, A., and Lettenmaier, D. P.: Long-range experimental hydrologic forecasting for the eastern United States, Journal of Geophysical Research: Atmospheres, 107, ACL 6–1–ACL 6–15, https://doi.org/https://doi.org/10.1029/2001JD000659, 2002.

Wood, A. W., Leung, L. R., Sridhar, V., and Lettenmaier, D.: Hydrologic implications of dynamical and statistical approaches to downscaling climate model outputs, Climatic change, 62, 189–216, 2004.

Wu, Q.: geemap: A Python package for interactive mapping with Google Earth Engine, The Journal of Open Source Software, 5, 2305, https://doi.org/10.21105/joss.02305, 2020.

Wu, X., Su, J., Ren, W., Lü, H., and Yuan, F.: Statistical comparison and hydrological utility evaluation of ERA5-Land and IMERG precipitation products on the Tibetan Plateau, Journal of Hydrology, 620, 129 384, https://doi.org/https://doi.org/10.1016/j.jhydrol.2023.129384, 2023.

Yamazaki, D., Ikeshima, D., Tawatari, R., Yamaguchi, T., O'Loughlin, F., Neal, J. C., Sampson, C. C., Kanae, S., and Bates, P. D.: A high-accuracy map of global terrain elevations, Geophysical Research Letters, 44, 5844–5853, https://doi.org/https://doi.org/10.1002/2017GL072874, 2017.

Yin, J., Guo, S., Gu, L., Zeng, Z., Liu, D., Chen, J., Shen, Y., and Xu, C.-Y.: Blending multi-satellite, atmospheric reanalysis and gauge precipitation products to facilitate hydrological modelling, Journal of Hydrology, 593, 125 878, https://doi.org/https://doi.org/10.1016/j.jhydrol.2020.125878, 2021.

Zemp, M., Huss, M., Thibert, E., Eckert, N., McNabb, R., Huber, J., Barandun, M., Machguth, H., Nussbaumer, S. U., Gärtner-Roer, I., Thomson, L., Paul, F., Maussion, F., Kutuzov, S., and Cogley, J. G.: Global glacier mass changes and their contributions to sea-level rise from 1961 to 2016, Nature, 568, 382–386, https://doi.org/10.1038/s41586-019-1071-0, 2019.

Zhang, Z., Liu, L., He, X., Li, Z., and Wang, P.: Evaluation on glaciers ecological services value in the Tianshan Mountains, Northwest China, Journal of Geographical Sciences, 29, 101–114, https://doi.org/10.1007/s11442-019-1586-1, 2019.

Zieliński, T. P.: IIR Digital Filters, pp. 193–226, Springer International Publishing, Cham, ISBN 978-3-030-49256-4, https://doi.org/10.1007/978-3-030-49256-4_8, 2021.

https://doi.org/10.5194/egusphere-2025-3461
Preprint. Discussion started: 15 December 2025

Table 1. MATILDA Model Parameters.

Parameter	Description	Unit	Range	Default
	Atmospheric Parameters			
lr_{temp}	Temperature lapse rate	°C m^{-1}	[-0.0065, -0.0055]	-0.006
lr_{prec}	Precipitation lapse rate	mm m^{-1}	[0, 0.002]	0
PCORR	Precipitation correction factor	-	[0.5, 2]	1.0
	Snow and Glacier Melt Parameters			
TT_{snow}	Threshold temperature for snow	°C	[-1.5, 1.5]	0
TT_{diff}	Temperature range for rain-snow transition	°C	[0.5, 2.5]	2
SFCF	Snowfall correction factor	-	[0.4, 1]	0.7
$CFMAX_{snow}$	Melt factor for snow	mm K^{-1} day^{-1}	[0.5, 10]	5
$CFMAX_{rel}$	Melt factor for ice relative to snow	-	[1.2, 2]	2
CWH	Water holding capacity of snowpack	-	[0, 0.2]	0.1
CFR	Refreezing coefficient	-	[0.05, 0.25]	0.15
AG	Control parameter of the glacier storage-release scheme	-	[0, 1]	0.7
	Soil and Evapotranspiration Parameters			
BETA	Shape coefficient for soil moisture routine	-	[1, 6]	1.0
CET	Correction factor for evapotranspiration	-	[0, 0.3]	0.15
FC	Field capacity of soil	mm	[50, 500]	250
LP	Fraction of field capacity for maximum evapotranspiration	-	[0.3, 1]	0.7
	Flow and Routing Parameters			
K_0	Recession coefficient for surface flow	day^{-1}	[0.01, 0.4]	0.055
K_1	Recession coefficient for intermediate groundwater flow	day^{-1}	[0.01, 0.4]	0.055
K_2	Recession coefficient for deep groundwater flow	day^{-1}	[0.001, 0.15]	0.04
PERC	Percolation rate from upper to lower groundwater reservoir	mm day^{-1}	[0, 3]	1.5
UZL	Threshold for quick flow from upper zone	mm	[0, 500]	120
MAXBAS	Length of triangular routing function	day	[2, 7]	3.0

https://doi.org/10.5194/egusphere-2025-3461
Preprint. Discussion started: 15 December 2025

Table 2. Default climate change indicators calculated as part of the MATILDA output. Definitions and customization options can be found in the module documentation.

Indicator	**Unit**
Month with Maximum and Minimum Precipitation	MoY[a]
Day of the Year with Maximum Flow	DoY[b]
Start, End, and Length of the Potential Melting Season	DoY[b], d
Potential and Actual Aridity	-
Number of Days in Dry Spells per Year	d
$q5$, $q50$, $q95$	mm
Average Frequency and Duration of Low/High Flow Events	a^{-1}, d
Climatic Water Balance	mm
SPI[c] and SPEI[d] (for 1, 3, 6, 12, and 24 months)	-

[a]MoY: Month of Year, [b]DoY: Day of Year,
[c]Standardized Precipitation Index, [d]Standardized Precipitation-Evapotranspiration Index

https://doi.org/10.5194/egusphere-2025-3461
Preprint. Discussion started: 15 December 2025

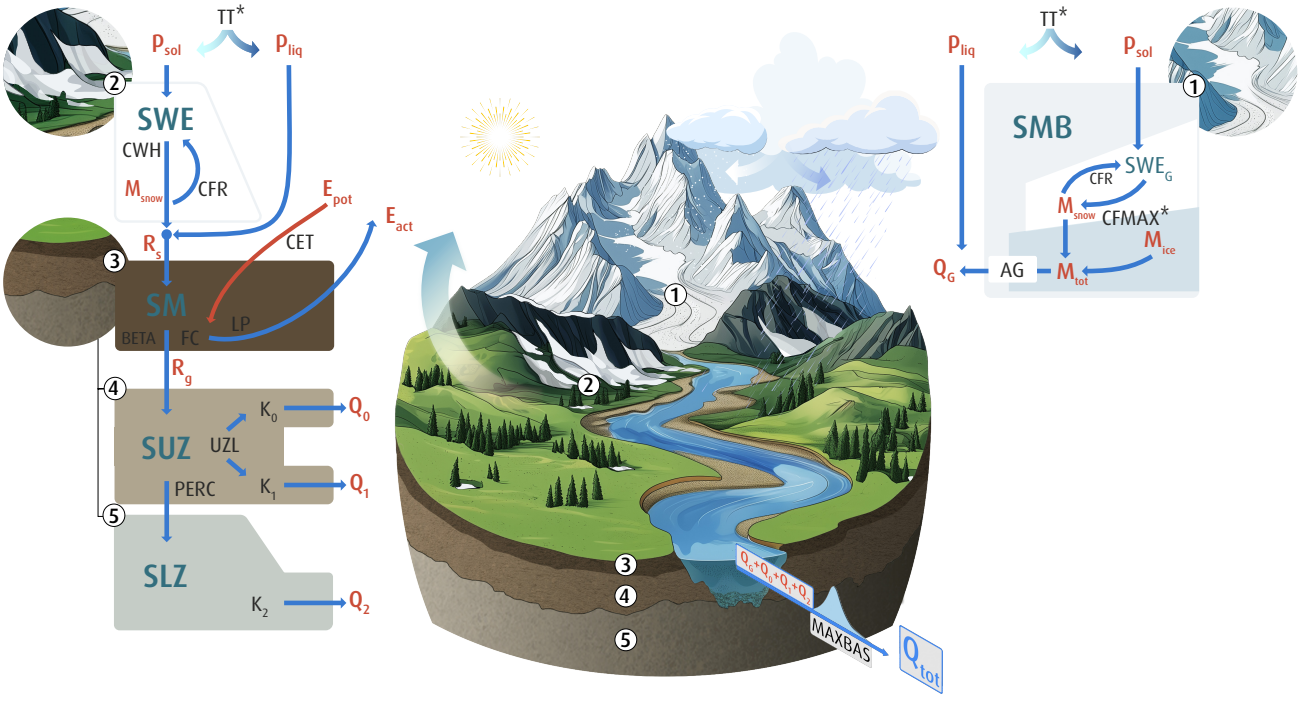

Figure 1. 'Cupcake scheme' of the MATILDA core routines. Numbers refer to hydrologic subdomains of the conceptual high-mountain landscape: (1) The glacier routine consisting of a temperature-index melt model with a Δh parametrization, (2) the temperature-index based snow routine, (3) the soil routine, (4) the upper and (5) the lower groundwater routine. Subdomains 2-5 are HBV standard routines. Reservoirs are written in teal blue, model parameters in black, fluxes in red. Parameters with an asterisk have two variants. Long names for parameters are listed in 1. Details on the processing and long names for reservoirs and fluxes are provided in the text.

https://doi.org/10.5194/egusphere-2025-3461
Preprint. Discussion started: 15 December 2025

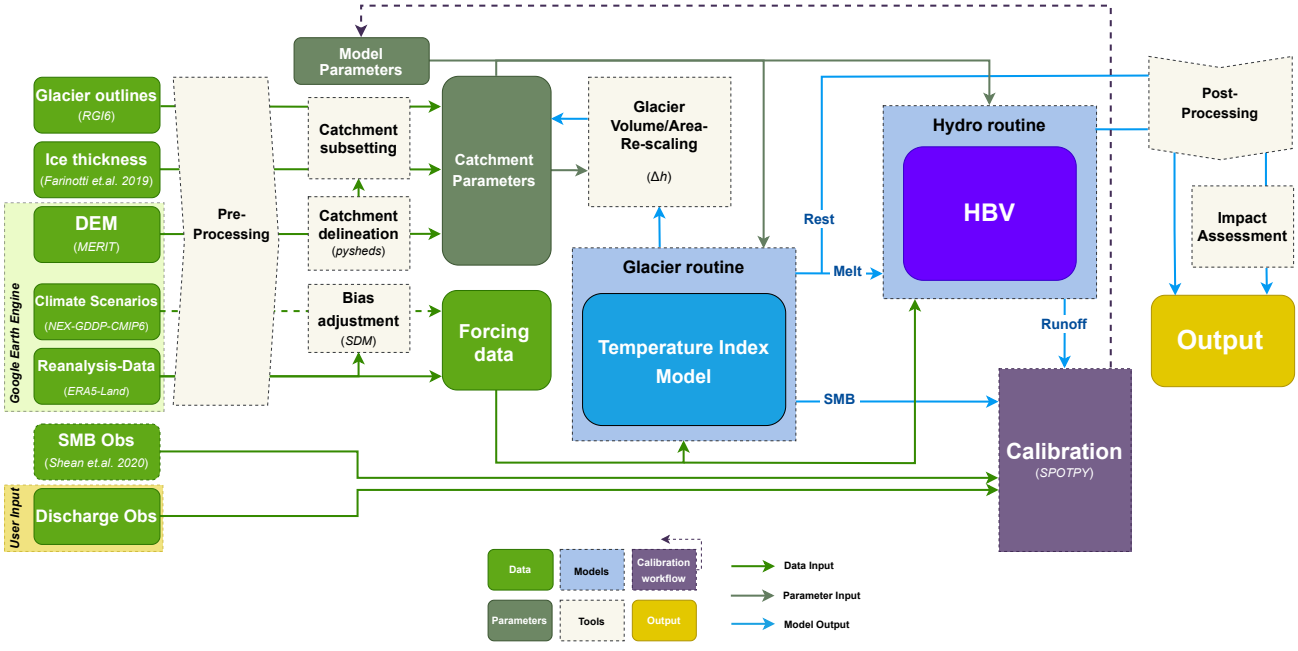

Figure 2. Flowchart illustrating the processing chain of the MATILDA workflow. The legend shows the color coding. Default datasets, software libraries, and methods are noted in parentheses. The respective sources are mentioned in the text.

https://doi.org/10.5194/egusphere-2025-3461
Preprint. Discussion started: 15 December 2025

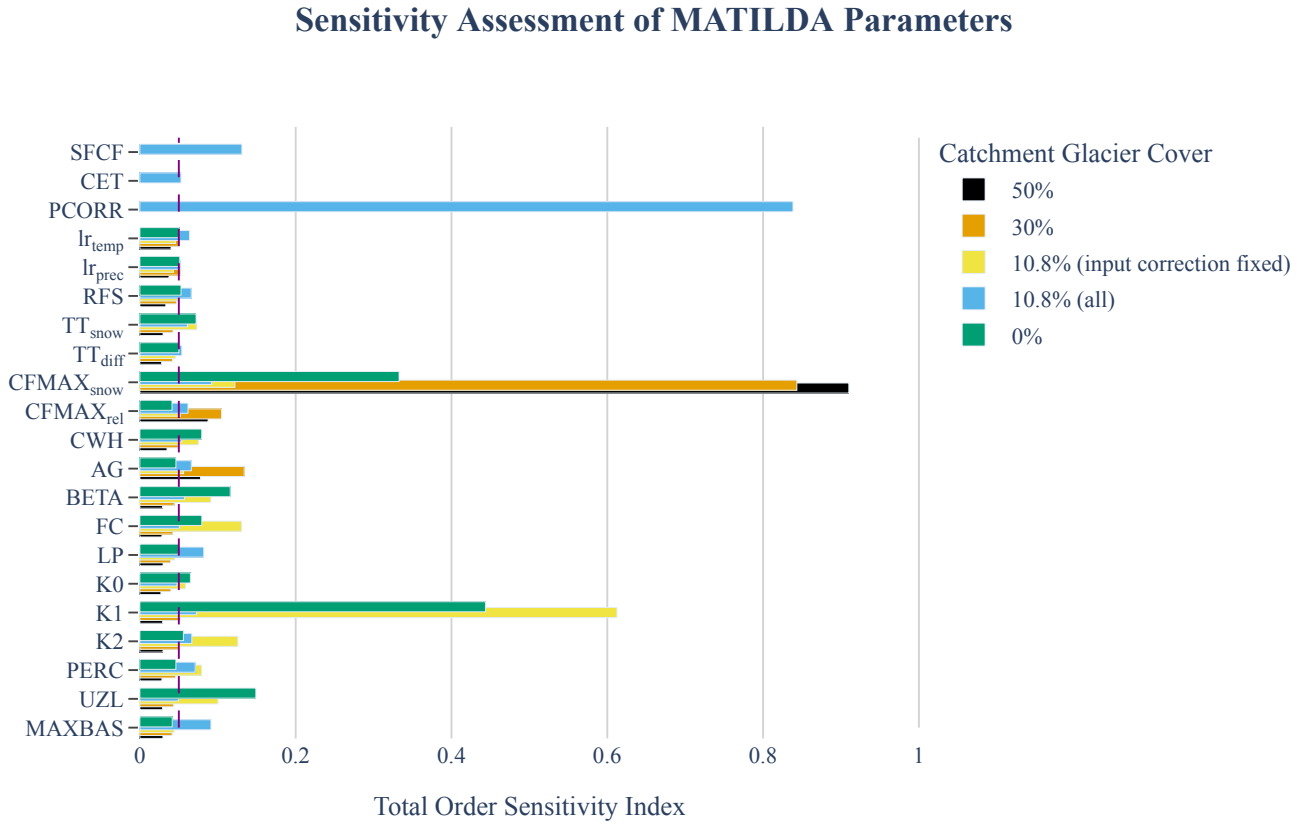

Figure 3. Results of five consecutive Fourier Amplitude Sensitivity Tests (FAST), each based on 1,500,012 random parameter samples for the period 2000-2017. Blue bars show the total order sensitivity index (S_T) of all MATILDA parameters for the benchmark catchment (see Schuster et al. (2025d)). Long names for parameters are listed in 1. Yellow bars show S_T for the internal parameters only (input correction parameters fixed). The other colors show S_T for the same catchment in three glacierization scenarios. The indicated fractions refer to the initial glacier cover in the year 2000, which was artificially changed from the original value (10.8 %) to 0 %, 30 %, and 50 %, respectively.